Quasioptical Millimeter-Wave Hybrid and Monolithic PIN Diode Switches

Karl D. Stephan, Frank H. Spooner, and Paul F. Goldsmith, *Fellow, IEEE*

***Abstract*—The PIN diode switch is an essential building block in many microwave and millimeter-wave systems. In this paper we report the development of a new type of quasioptical PIN diode switch. First, we briefly describe the quasioptical imaging application which motivated the development of the switch. Next, we explain the theory of switch operation in both its reflection and transmission modes. We present experimental results from measurements of both hybrid and monolithic circuits in the millimeter-wave range. The hybrid version exhibits losses in the reflection mode of 1 dB or less and isolation of 20 dB or more. Performance of the monolithic version is comparable, despite a PIN diode yield of less than 80%.**

I. Quasioptical Imaging Application: Dicke Switch

RADIOMETRIC imaging systems operating around 94 GHz have shown promise in numerous remote sensing applications. For example, fog that is opaque to visible or infrared light can be penetrated by aircraft landing aids using millimeter-wave imaging rediometers. Recently published experimental images [1], [2] show reasonably good contrast, but only if care is taken to compensate for the gain drift in the receiver channels, which can show up as noise in the image. One standard technique to compensate for drift is the Dicke switch. This switch is placed between the receiver and the source of radiation whose effective temperatures is to be measured. At periodic intervals, the Dicke switch transfers the receiver input to a matched load at a known reference temperature, allowing continuously updated calibration of the receiver gain. This switching is typically performed at a rate in the audio-frequency range (10-1000 Hz).

Since the Dicke switch is usually the first active component the signal encounters, its loss must be kept to a minimum. However, high-speed, high-resolution imaging will require an array of many receivers, all operating simultaneously. Since a single low-loss waveguide switch can cost thousands of dollars and occupy several cubic centimeters, it is difficult to provide a separate Dicke switch and load for each receiver channel in a multi-channel imaging system. One way to solve this problem is to place a quasioptical Dicke switch in front of the entire receiver array, as shown in Fig. 1.

This quasioptical switch must perform two functions. In its reflection state, it must reflect an incoming wavefront from the imaging optics to the receiver array, with as little loss as possible. In the transmission state, it must pass the thermal emission from the reference temperature load to the receiver array. In one system developed at Millitech Corporation, the essential Dicke switching function was performed by a rotating mechanical component, but size, weight and vibration problems make an all-electronic switch preferable. The quasioptical PIN diode switch we will now describe has been developed for this application.

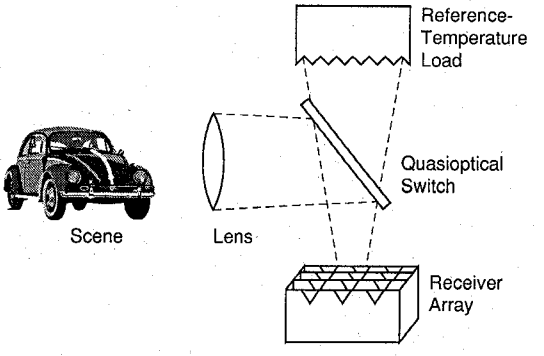

Fig. 1. Schematic plan of millimeter-wave camera using quasioptical switch to expose receiver array alternately to scene and reference temperature load.

II. Design Theory

The heart of the switch design is an array of PIN diodes embedded in a conducting metal grid. Diode grids have demonstrated quasioptical functions such as phase shifting [3] and frequency multiplication [4], and the basic theory of operation is fairly well understood.

As long as the period of a rectangular grid is less than a free-space wavelength, a simple equivalent circuit analysis can predict its transmission and reflection of waves normally incident upon it [5]. Suppose a thin perfectly conducting metal mesh lies at the interface between two dielectrics. Let the dielectrics have indices of refraction n_1 and n_2. As Fig. 2(a) shows, the mesh period is g and the conductor trace width is $2a$. For a linearly polarized plane wave normally incident upon the mesh, free space can be modeled as a transmission line of impedance $Z_S = [\mu_o/\varepsilon_o]^{1/2}$, where μ_o and ε_o are the permeability and permittivity of free space, respectively. If the medium's index of refraction is n, the equivalent impedance is reduced by that factor, as indicated in the equivalent circuit of Fig. 2(b). Since the electric field is continuous across thin mesh, the corresponding equivalent circuit is composed of shunt elements only. Let us define a normalized frequency $\omega = g/\lambda_o$, where λ_o is the free-space wavelength. At a

Manuscript received September 8, 1992; revised April 15, 1993.

K. D. Stephan was with Millitech Corporation on leave from the University of Massachusetts at Amherst, Amherst, MA 01003.

F. H. Spooner was with Millitech Corporation. He is now with American Holographic, Littleton, MA 01460.

P. F. Goldsmith was with Millitech Corporation. He is now with the Department of Astronomy, Cornell University, Ithaca, NY, 14853.

IEEE Log Number 9211934.

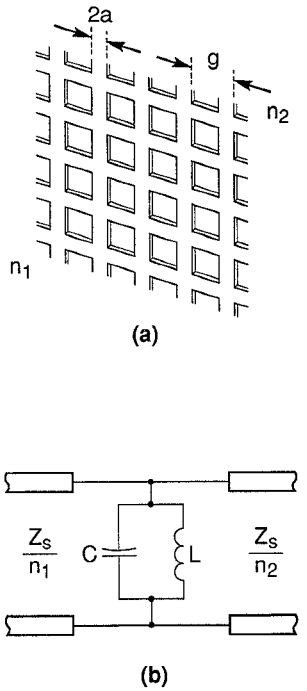

Fig. 2. (a) Perfectly conducting metallic mesh with grating period g and trace width $2a$. (b) Equivalent circuit of mesh.

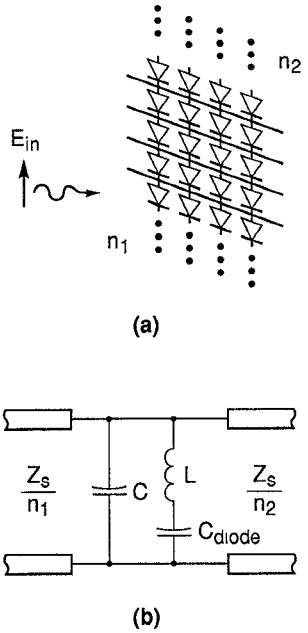

Fig. 3. (a) Mesh with diodes in OFF state, inserted into vertical traces. (b) Equivalent circuit of mesh with diodes in OFF state.

normalized frequency ω_o (typically unity), a parallel resonance occurs for a free-standing mesh, and it transmits incident energy with no reflection loss. For a mesh at the interface between two dielectrics of indices n_1 and n_2, the parallel-resonant frequency changes to

$$\omega_0' = \omega_0 \left[\frac{2}{n_1^2 + n_1^2}\right]^{\frac{1}{2}} \tag{1}$$

Using this definition, Whitbourn and Compton found that the equivalent circuit inductor L's reactance X_L and the capacitor C's reactance X_c are given by

$$\frac{X_L}{Z_S} = -\left(\omega_0' \ln \csc \frac{\pi a}{g}\right)\left(\frac{\omega}{\omega_0'} - \frac{\omega_0'}{\omega}\right)^{-1} \tag{2}$$

and

$$\frac{X_C}{Z_S} = \frac{2}{n_1^2 + n_2^2}\left(4\omega_0' \ln \csc \frac{\pi a}{g}\right)^{-1}\left(\frac{\omega}{\omega_0'} - \frac{\omega_0'}{\omega}\right) \tag{3}$$

Although these expressions are based on an empirically modified quasistatic analysis, they agree reasonably well with measurements up to the parallel-resonant frequency of the mesh. If the frequency range of interest is limited to a band sufficiently below ω_0, values for L and C in Fig. 2 can be calculated from their respective reactances X_L and X_C in (2) and (3) by using a nominal center frequency. The grid used in our experiments did not have the rectangular mesh pattern assumed in the above analysis. Nevertheless, the behavior of our grid is qualitatively similar to that of the theoretical rectangular mesh grid. The preceding analysis provides a good starting point for empirical modifications of the grid element shape.

A. Reflection Design

Now suppose we insert a PIN diode in the OFF state (no DC current flowing) into each vertical trace in the mesh, as shown in Fig. 3(a). If the incident wave's electric field is parallel to the diodes, the current induced in the vertical traces must now pass through the diodes, as the equivalent circuit of Fig. 3(b) shows. The diode's impedance in the OFF state is primarily capacitive, represented by C_{diode}. As long as the mesh is square and there is one diode per period, the equivalent circuit C_{diode} is the actual capacitance per diode. The diode capacitance C_{diode} is not to be confused with the mesh capacitance C discussed above.

Once the diodes are inserted into the mesh, a series resonance will appear at a frequency below the mesh's parallel resonance. The series resonance appears at a frequency f_S (not normalized) given approximately by

$$f_S = 1 \Big/ \left(2\pi [LC_{\text{diode}}]^{\frac{1}{2}}\right) \tag{4}$$

At this series resonant frequency f_S, a lossless mesh with purely capacitive diodes will act as a perfect reflector, since the mesh's inductive reactance cancels the diode's capacitive reactance. Losses in the mesh or diode series resistance will cause some absorption and transmission, but since the series resistance of PIN diodes in the OFF state is generally lower than it is in the ON state (forward bias with DC current flow), losses can be kept low. This series resonance is the basis for the reflection mode of the quasioptical PIN diode switch.

PIN diode arrays have been used previously for waveguide switching at millimeter wavelengths, as reported by Armstrong, *et al.* [6] Such waveguide arrays depend upon the low forward bias resistance of the diodes for high transmission isolation. Low transmission loss with the diodes OFF is achieved by a parallel-tuned circuit made up of diode capacitance and a shunt inductive iris on the array substrate. Although there

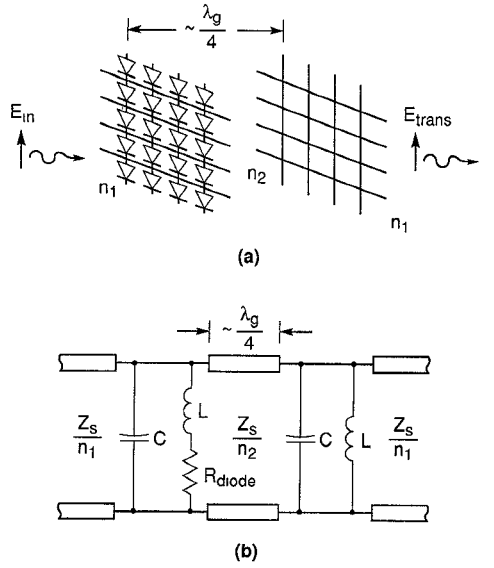

Fig. 4. (a) PIN diode mesh backed by passive mesh on backside of substrate. (b) Equivalent circuit of mesh-substrate-mesh-sandwich.

is a superficial resemblance between Armstrong's waveguide array and our quasioptical array, the modes of operation are quite different. The quasioptical array uses a series resonance to achieve low reflection loss, while the waveguide array uses a parallel resonance to obtain low transmission loss. In both cases the diodes are OFF.

B. Transmission Design

When a PIN diode is forward-biased, the terminal impedance of the device is dominated by the hole-electron plasma in the I-region, which appears resistive above a few tens of MHz. This resistance is inversely proportional to DC bias current down to a limit determined by carrier lifetime and parasitic resistances. Let this minimum practical resistance when the diodes are forward-biased in the ON state be R_{diode}. A single grid with forward-biased diodes does not give sufficiently large transmission for practical uses. In order to achieve adequate transmission through the mesh with the diodes ON, additional components are needed.

Suppose a second mesh is placed on the back side of the substrate that supports the first PIN diode mesh, as shown in Fig. 4(a). This second mesh has no PIN diodes and unbroken conductors, so its equivalent circuit has no R_{diode}, as Fig. 4(b) shows. If the electrical length of the substrate is approximately one-quarter of a wavelength in the substrate material ($\lambda_g/4$), the reflection from the second mesh will combine with the reflection from the first mesh to cause substantial cancellation of the total reflection. This scheme allows perfect transmission only when there are no losses, but for reasonably small values of R_{diode} on-resistance, substantial transmission can occur.

The reactance contributed by the meshes' inductance means that the substrate thickness for zero loss is no longer exactly an electrical quarter-wavelength. We have developed proprietary quasioptical array analysis software based on a paper by Saleh [7]. This software calculates transmission and reflection characteristics of a stack of meshes and dielectric spacers. To design a circuit for use at a particular frequency, we iteratively adjust the dielectric thickness of the software model to give minimum loss at the design frequency. In the laboratory, thin shims of quartz or other low-loss dielectric are combined to approximate the theoretical thickness required.

When the diodes switch from ON to OFF, the reflection mode in the OFF state is unaffected by the presence of the second mesh, so the transmission mode can be optimized more or less independently of the reflection mode.

The final product of the design is a planar "sandwich" consisting of an active mesh with PIN diodes, a dielectric spacer of a prescribed thickness, and a passive metal-only mesh. When the diodes are in the OFF state, waves incident on the diode mesh are reflected with very low loss. When the diodes are forward-biased into the ON state, most of the incident radiation is transmitted, with relatively low reflection and absorption loss.

III. Hybrid Circuit

The practical design of this type of quasioptical PIN diode switch is determined by the minimum diode capacitance C_{diode} in the OFF state. For a given series resonant design frequency f_S, a low diode capacitance means that a relatively high mesh inductance L can be tolerated. Since L is directly proportional to the mesh period g (this is true for any shape of periodic mesh, not just the pattern of Fig. 1), a large L allows a larger mesh period, within the constraint of keeping g smaller than a free-space wavelength.

A large mesh period means fewer diodes per unit area. A diode forward current of 5 mA is typically required to achieve low series resistance. The resulting 5 mW of power dissipation per diode can quickly lead to an unacceptably high thermal load if the diode density is too great. This is why the minimum diode density that will provide acceptable electrical performance should be used. Other quasioptical diode arrays such as those described by Sjogren, *et al.* [8], used Schottky diodes, whose lower power dissipation allowed greater diode density. We feel that arrays of PIN diodes will have a much greater ultimate power handling capacity and freedom from nonlinear effects that may trouble Schottky diode arrays.

For the hybrid design, we chose an alumina substrate with a relative dielectric constant ε_r of about 9.5 ($n = [\varepsilon_r]^{1/2} = 3.1$). Alumina provides a mechanically rugged base on which to bond beam lead PIN diodes. The manufacturer of the silicon diode we selected [9] cites a typical OFF state capacitance of 17 fF. For a series resonance at $f_S = 94$ GHz, (4) gives a required mesh inductance of 169 pH. Depending on precisely how the diode capacitance is defined, values other then 17 fF can be measured, and this will affect the calculated mesh inductance accordingly.

When one attempts a diode array design based on the classical rectangular grid treated by (1) and (2), a difficulty arises. If one chooses a mesh period g to give an acceptably low diode density, a mesh showing low enough inductance to be used with available diodes turns out to be "fat". That is, the ratio of strip width $2a$ to period g can exceed 0.5. This

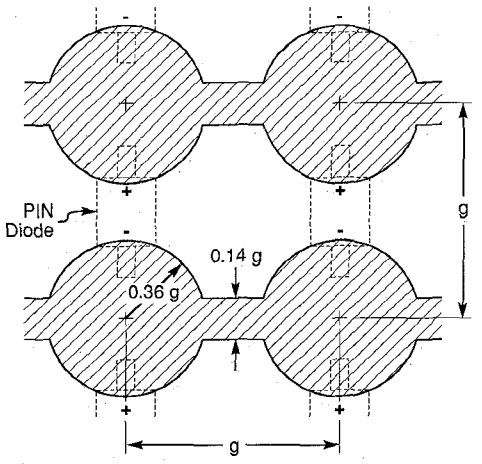

Fig. 5. Mesh pattern used in hybrid quasioptical PIN diode switch (g = 0.89 mm).

shape presents layout and interconnection problems with the kinds of diodes we use.

Instead, we experimented with grids having acceptably thin strips at the diode locations. To achieve lower inductance we expanded the conductor into octagonal or circular patches centered at the intersection of the original thin mesh strips. While these complex shapes cannot be analyzed directly using (1) and (2), such meshes do exhibit the same general parallel-resonant behavior as the classical rectangular mesh. With enough experimental data one can work backward and derive an effective strip width $2a$ for a complex mesh of period g. This is in fact how the mesh pattern shown in Fig. 5 was designed. Since the experiments to be presented show a series resonance near 94 GHz, we feel that our original design goal of 169 pH mesh inductance was achieved.

A. Fabrication

The quasioptical test setup to be described below creates a Gaussian beam [10] whose phase front is approximately planar and whose amplitude falls to about 1% of the on-axis value at a radius of 1.25 cm from the axis. This beam radius means that the smallest diameter circuit that could be tested accurately is about 2.5 cm. Accordingly, a circular hole about 2.3 cm in diameter was filled with the repeated pattern of Fig. 5, in which g = 0.89 mm. The resulting overall pattern is shown in Fig. 6. It has spaces for 464 diodes, which were bonded to the chrome-gold conducting pattern using conventional manual bonding techniques. Bias was applied to the top and bottom conducting strips in a series-parallel arrangement. Although this meant that the average bias current for the top and bottom rows of diodes was about three times that of the middle row, no ill effects from this unbalance were noted.

To finish the circuit, the substrate with the active devices must be backed by a dielectric spacer and a passive mesh whose diodes were replaced by short circuits, as indicated in Fig. 4. We found that the pattern of Fig. 5 without diodes worked well in this application when rotated 90°, so that the metallic traces took the place of the diodes. This rotated pattern was used on the passive substrate, and a fused silica spacer of a suitable thickness was inserted between the active and passive

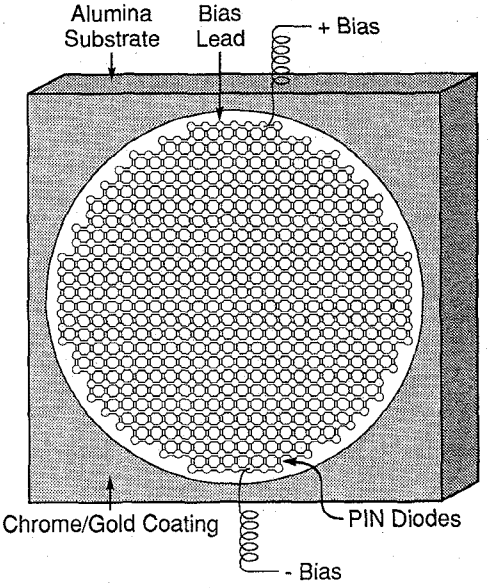

Fig. 6. Overall view of hybrid switch, showing chrome-gold pattern with diodes on alumina substrate.

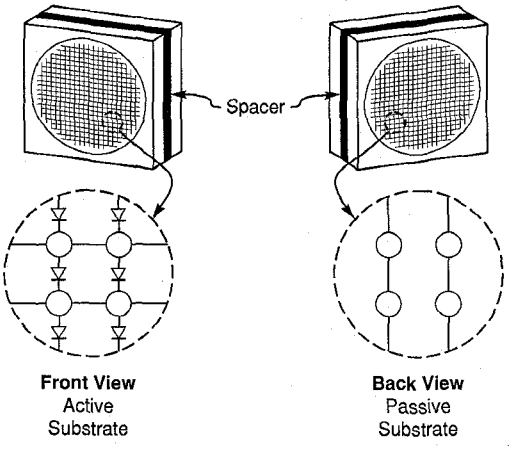

Fig. 7. View of active substrate, spacer layer and passive substrate, showing relative orientation of meshes.

TABLE I
SWITCH SUBSTRATES AND SPACERS

Type of Switch	Active Substrate		Spacer		Passive Substrate	
	Material	Thickness (mm)	Material	Thickness (mm)	Material	Thickness (mm)
Hybrid	Alumina $\varepsilon_r = 9.5$	0.25	Fused Silica $\varepsilon_r = 3.8$	0.15	Alumina $\varepsilon_r = 9.5$	0.25
Monolithic	GaAs $\varepsilon_r = 13$	0.50	GaAs $\varepsilon_r = 13$	0.49	GaAs $\varepsilon_r = 13$	0.50

substrates to give the proper electrical distance between the two meshes. The completed assembly is shown in Fig. 7, and the thicknesses of the components are given in Table I.

B. Testing and Results

A schematic of the Gaussian beam setup used to test the quasioptical PIN diode switch is shown in Fig. 8. For the hybrid circuit tests, lenses of 7.5 cm diameter and 7.5 cm focal

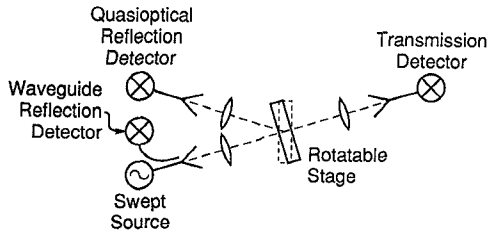

Fig. 8. Quasioptical reflection and transmission test setup.

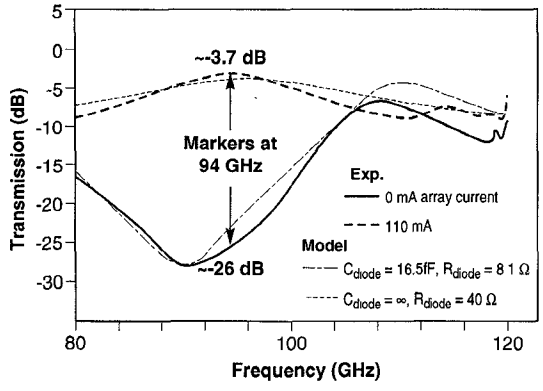

Fig. 9. Measured and modelled hybrid switch transmission loss, OFF (solid line) and ON (dashed line).

length were used to create a beam with a waist radius of about 0.6 cm. Antireflection coatings reduced reflections from the fused silica lenses. Focusing lenses were necessary because the unfocused free-space reflection from the relatively small switch would have been too weak to measure in comparison to the reflections from its support structure.

For the transmission tests, the 0 dB reference was taken as the loss of the setup with no switch inserted in the beam. Residual reflections between the lenses caused a rapid oscillation of the frequency response, which was eliminated by means of the 5% smoothing function on the scalar network analyzer. Fig. 9 shows the transmission response measured with the beam normally incident onto the hybrid switch. With no bias (diodes in the OFF state), the series resonance fs occurred at about 90.3 GHz, and the loss exceeds 20 dB over a 12 GHz bandwidth. Loss at the design frequency of 94 GHz is 26 dB in the OFF state. When the diodes were turned ON, a minimum loss of 3.7 dB was measured at 93.9 GHz. At a total bias current of 110 mA, the transmission loss was still decreasing with increasing bias. At this current, the circuit was dissipating about 2.2 W and slight thermal instability was beginning to show as an upward drift in bias current for a constant bias voltage. At the total current level of 110 mA, the average current per diode varied from 15.7 mA in the top and bottom rows to 4.4 mA in the center. The manufacturer's typical specifications state that the diode resistance corresponding to this current range is from about 5 to 15 ohms at 100 MHz.

We modelled this circuit using the parameters given in Table I. With 0.03 mm airgaps added between the layers and the diode parameters adjusted to the values shown, we were able to model the experimental results. Agreement is reasonably good in the frequency range of interest. The

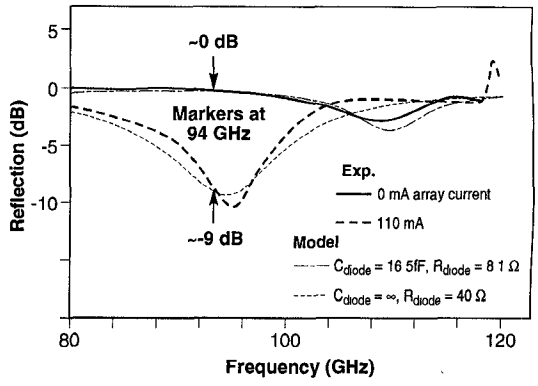

Fig. 10. Measured and modelled hybrid switch reflection loss, diodes OFF (solid line) and ON (dashed line).

relatively high R_{diode} on-resistance of 40 ohms, compared to the manufacturer's typical value of 5 to 15 ohms for these current levels, can be accounted for by the increase in skin resistance and parasitic loss between 100 MHz and 94 GHz.

For the reflection measurement, the switch holder was tilted so that the angle of beam incidence was 17°. This allowed a third lens and horn setup to measure the reflected energy quasioptically. The 0 dB reference was chosen to be the reflection from an aluminum plate held nearly at the same location as the quasioptical switch. Because of positioning errors, diffraction, and other problems, we believe that the accuracy of this reflection measurement is only ±0.5 dB. Strictly speaking, the equivalent circuit model we used for design is not valid for angles of incidence other than normal (perpendicular to the array). However, we feel that for this type of circuit the difference in behavior with angles of incidence between 0° and 17° is small.

Fig. 10 presents the reflection data and modelled results for the hybrid quasioptical switch. With the diodes in the OFF state (no bias), the measured reflection loss is approximately 0 dB. The actual loss was too small to measure accurately. Since the reflection mode loss is the more critical one in the imaging application, this low reflection loss is a good result. With the diodes ON, the reflection loss at 94 GHz increases to 9 dB, peaking at about 12 dB. Ideally infinite reflection loss is desired, but this figure could be improved with a secondary matching layer on top of the active substrate. The same model used for the transmission data gave acceptable agreement to the reflection data as well.

These encouraging results from the hybrid quasioptical switch led us to develop a monolithic version with large-volume production in mind. Although work on the monolithic switch is still in progress, the preliminary results obtained are encouraging, as the following discussion will show.

IV. Monolithic Circuit

The hybrid circuit was copied as closely as possible in the monolithic circuit design. To the extent possible, the array period and all other dimensions were kept the same. There were two major differences, however. In order to simplify DC testing and diagnostics, we decided to lay out a square array of 25 × 25, or 625 diodes, rather than the circular hybrid pattern.

The other difference was that the beam lead silicon diodes were replaced with vertical monolithic PIN diodes fabricated in the same process as the mesh pattern.

A. Fabrication

The array of 625 PIN diodes was fabricated as one large device consisting of 25 rows of 25 diodes each. The entire array was approximately 2.2 cm square. Gold-plated pads at opposite corners of the array provided DC biasing connections to gold wire bonds.

Processing began with vendor-supplied OMCVD-grown N^+, I, and P^+ layers on top of semi-insulating GaAs. We then evaporated Au/Ag/Zn P^+ ohmic metal and lifted it off using an image reversal photoresist procedure. Two wet chemical etch steps followed. The first etched down to the middle of the I layer, defining the diode active regions. The second etch removed 10 microns of GaAs to define mesas that isolated the diodes electrically from each other at DC. We etched through the I layer to form the N^+ ohmic contacts, using a liftoff process with Ni/Au/Ge/Au metallization. Both ohmic metals were alloyed using a rapid thermal processor.

Photoresist served to pattern the circuit metal interconnects. We lifted off a sputtered layer of Ti/Mo/Au which connected all the diodes into the series-parallel DC bias circuit. We passivated the device with silicon dioxide deposited with an ultraviolet chemical vapor deposition process. Photoresist was used to support the airbridges and define the passivation etch. We sputtured a thin Ti/Au contact layer all over the wafer, and patterned it with photoresist so that 2–3 microns of Au plated the airbridges selectively. The airbridges connected the P^+ contacts to the circuit metal. We then removed the unwanted photoresist and metal layers and DC-tested the device row by row. A typical yield of nonshorted devices was about 80%. We disconnected shorted devices from the array by mechanically removing their airbridges. The diodes thus opened did not contribute to the RF operation of the circuit, but were prevented from shorting out the DC bias of the remaining functional diodes in their row. Fig. 11 shows an SEM photograph of a typical PIN diode, and Fig. 12 is an SEM photo of a portion of the array.

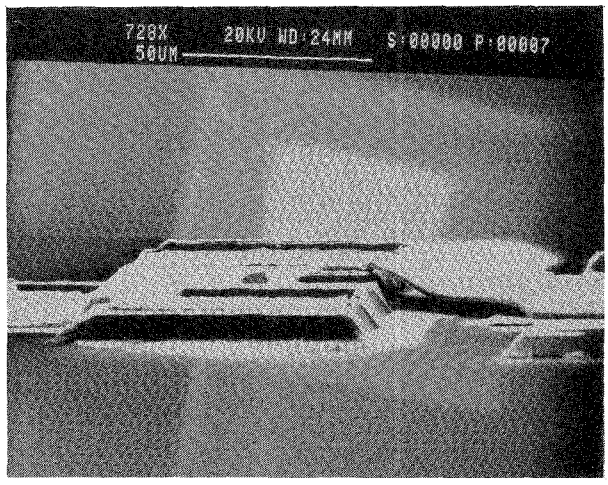

Fig. 11. Scanning Electron Microscope (SEM) photograph of vertical PIN diode and airbridge used in monolithic switch.

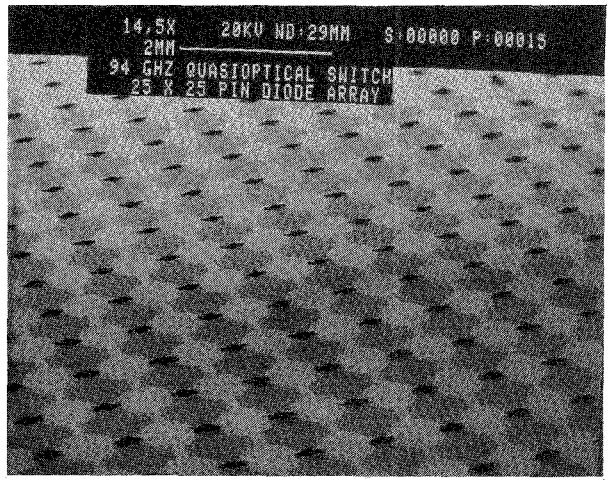

Fig. 12. SEM photograph of portion of monolithic array.

B. Tests

Preliminary tests [11] of the monolithic switch showed that the series resonance f_S was around 70 GHz. Assuming that the mesh inductance for the hybrid and the monolithic switches are the same, this frequency shift would be accounted for by an increase in diode capacitance to 17 fF $\cdot$ $(94/70)^2$ = 31 fF. This figure is consistent with both low frequency measurements and the capacitance required in our RF model to match experimental data. Further work is required to lower the monolithic diode capacitance.

Since the original quasioptical test setup did not work below 75 GHz, another one for the 50–75 GHz range was built with Teflon lenses. The short focal length (2.3 cm) required to maintain a small beam waist with available horns meant that there was no room to perform a quasioptical reflection measurement. Instead, a waveguide directional coupler at the transmitting horn was used to measure reflections that reentered the horn. This technique is less accurate than the quasioptical reflection method. Fig. 8 shows the location of the waveguide reflection detector. For these 50–75 GHz tests, the quasioptical reflection detector and its lens were not present, although the two other lenses were still needed.

Unlike the hybrid tests results, the monolithic results were not corrected for empty-setup loss. The reason for this is shown in Fig. 13, which shows the measured transmission loss of the 50–75 GHz setup. Reflections between the lenses caused the ripple shown, which could not be meaningfully compensated. The setup loss averages about 2 dB. This figure should be subtracted from the following transmission and reflection data to arrive at an estimate of the actual performance of the monolithic switch.

Fig. 14 shows the reflection loss of the monolithic switch. The 0 dB reflection reference is a waveguide short. The average reflection loss in the zero bias state is low, less than 3 dB, although there is a dip around 70.6 GHz. (This dip appears to be related to reflection problems from the setup lenses.) Upon forward biasing the array of diodes to 143 mA forward current, the reflection loss increases by about 5 to

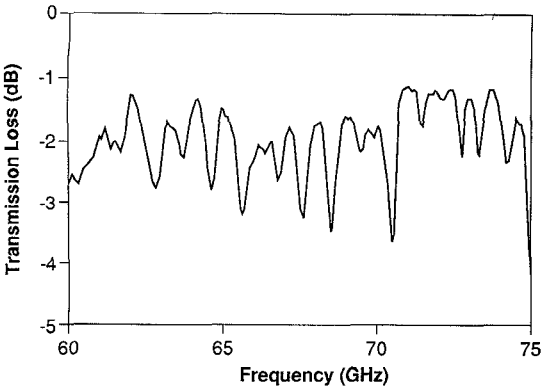

Fig. 13. Measured transmission loss of empty 50–75 GHz quasioptical test setup.

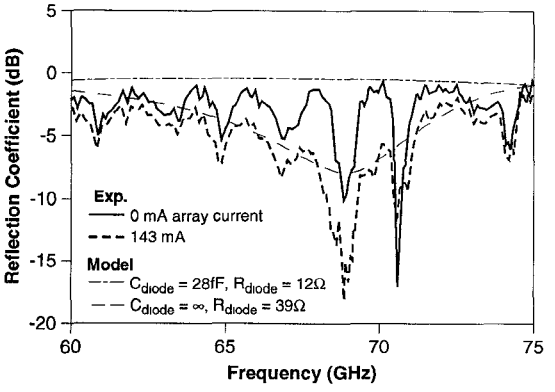

Fig. 14. Measured and modelled waveguide reflection loss of monolithic switch, for forward bias of 0 mA and 143 mA.

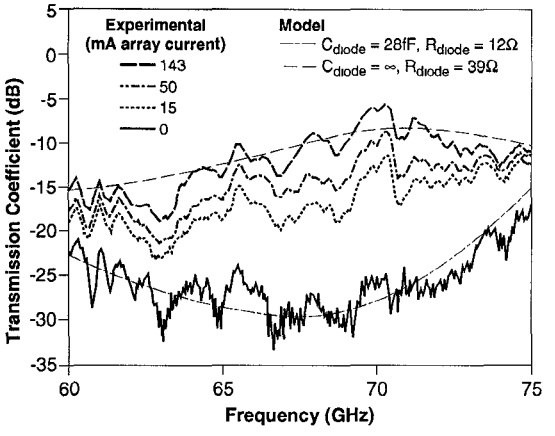

Fig. 15. Measured and modelled transmission loss of monolithic switch in test setup, for forward bias of 0 mA, 15 mA, 50 mA and 143 mA.

7 dB in the 65 to 70 GHz range. This forward bias current corresponds to average current per diode of 5.7 mA.

Since the monolithic tests were performed at normal incidence, we could apply the results of our equivalent circuit analysis software to them. By adjusting the values of C_{diode} and R_{diode} to best fit the experimental curves for reflection and transmission, we could arrive at estimates for these values in the monolithic circuit. This was the method used to derive the theoretical curves labeled "model" in Figs. 14 and 15.

The performance of the monolithic switch is easier to see in its transmission response, shown in Fig. 15. With the diodes OFF, loss peaks at about 30 dB near 70 GHz, referred to a waveguide-thru 0 dB reference. When increasing forward bias is applied, the transmission loss falls to an absolute minimum of 6 dB for 143 mA forward bias, with an average closer to 8 dB. Subtracting 2 dB for setup losses gives a minimum average transmission loss of around 6 dB. The theoretical model that gives the approximate best fit curves uses a forward bias diode having $C_{\text{diode}} = \infty$ and $R_{\text{diode}} = 39$ ohms. The zero bias diode model uses $C_{\text{diode}} = 28$ fF and $R_{\text{diode}} = 12$ ohms. These values for the monolithic diode capacitance are consistent with low frequency measurements we have performed.

This is encouraging performance, especially when yield is taken into account. Of the 625 devices originally fabricated on the monolithic switch, 129 were observed visually to be shorted, and their airbridges were removed by hand. Therefore, the maximum yield for the circuit's diodes is only (625-129)/625 or 79%, and it is likely that fewer diodes than this actually work. The overall circuit nevertheless works reasonably well. Although graceful degradation in the face of individual element failure is not a universal feature of quasioptical circuits, this diode switch appears to be relatively robust. DC power consumption with 143 mA forward bias was about 4.2 W. No thermal problems were noted with the substrate mounted in its aluminum holder.

A word about switching speed is in order. Although we did not measure the switching speed of the monolithic array, the relatively thin I-layer in the PIN diodes used means that the theoretical diffusion-limited switching time is on the order of 1 nsec. The series-parellel bias circuit currently in use would probably limit the maximum switching speed to slower values than this. In an application where switching speed was critical, an all-parallel bias circuit with a high current driver circuit would be more suitable.

V. Conclusion

We have shown that a quasioptical PIN diode switch can be designed using elementary plane wave equivalent circuit principles. We have demonstrated a hybrid switch that shows very low reflection loss at 94 GHz, and we have made progress in developing a monolithic version to perform a similar function. Although diode capacitance must be reduced in the monolithic version and diode yield needs to be higher, the data shows that the design is tolerant of the failure of individual devices.

The switches we discussed were tested with only a single receiver channel and a single incident beam. In the intended application of a multiple-channel receiver, each diode would be reflecting part of each of many beams arriving at angles of incidence varying from 0° up to 17°. The effects of diode resistance nonuniformity or individual diode failure in an imaging system are hard to predict. What we can say is that for a typical optical design there would not be a pixel-for-diode correspondence, since each diode would be acting on energy that affects many pixels. It is more likely that individual diode

failure would cause a less noticeable spread-out degradation in overall image quality.

In addition to the Dicke switch application for imaging systems, quasioptical diode switches should have the desirable property of high power operation. Although no experiments in this area have yet been performed, we have made some initial calculations. These estimates show that the switch studied should be able to isolate peak power in the multi-kilowatt range, with somewhat lower capability in transmission. Applications for switchable shielding and receiver protection at lower frequencies are also possible, since the diode array in the OFF state becomes mostly transparent below the millimeter-wave range.

ACKNOWLEDGMENT

We gratefully acknowledge the assistance of Gary P. Dion for bonding diodes, John W. LeBlanc for precision assembly, John J. Nicholson and John D. Williams for processing work, Edward Wong for machining assistance, Sudarsanam Bandla and G. Richard Huguenin for support and encouragement, and the reviewers for their helpful comments and suggestions.

REFERENCES

[1] W. W. Lam, P. Lee, L. Yujiri, J. Berenz and J. Pearlman, "Millimeter-wave imaging using preamplified diode detector," *IEEE Microwave Guided Wave Lett.*, vol. 2, pp. 276–277, July 1992.

[2] J. Brown, "Millimeter waves aid commercial applications," *Microwaves and RF*, pp. 113–116, July 1992.

[3] W. W. Lam, C. F. Jou, H. Z. Chen, K. S. Stolt, N. C. Luhmann, Jr. and D. B. Rutledge, "Millimeter-wave diode grid phase shifters," *IEEE Trans. Microwave Theory Tech.*, vol. 36, pp. 902–907, May 1988.

[4] C. F. Jou, W. W. Lam, H. Z. Chen, K. S. Stolt, N. C. Luhmann, Jr. and D. B. Rutledge, "Millimeter-wave diode grid frequency doubler," *IEEE Trans. Microwave Theory Tech.*, vol. 36, pp. 1507–1514, Nov. 1988.

[5] L. B. Whitbourn and R. C. Compton, "Equivalent circuit formulas for metal grid reflectors at a dielectric boundary," *Applied Optics*, vol. 24, pp. 217–220, Jan. 15, 1985.

[6] A. L. Armstrong, D. E. Wheeler and J. Goodrich, "High power broadband, 35 GHz waveguide switch using a monolithic diode array," 1984 *IEEE MTT-S Int. Microwave Symp. Dig.*, San Francisco, CA, May 30–June 1, 1984, pp. 400–401.

[7] A. A. M. Saleh, "An adjustable quasioptical bandpass filter-part I: theory and design formulas," *IEEE Trans. Microwave Theory Tech.*, vol. MTT-22, pp. 728–739, July 1974.

[8] L. B. Sjogren, H-X. L. Liu, F. Wang, T. Liu, W. Wu, X-H. Qin, E. Chung, C. W. Domier, N. C. Luhmann, Jr., J. Maserjian, M. Kim, J. Hacker, D. B. Rutledge, L. Florenz, and J. Harbison, "Monolithic millimeter-wave diode array beam controllers: theory and experiment", *Third Int. Symp. on Space Terahertz Technology*, Ann Arbor, MI, Mar. 24–26, 1992, pp. 45–57.

[9] Hewlett-Packard No. HPND-4005.

[10] P. F. Goldsmith, "Quasi-optical techniques at millimeter and submillimeter wavelengths", Chapter 5 in Vol. 6 of *Infrared and Millimeter Waves*, Kenneth J. Button, Ed., New York: Academic Press, 1982, pp. 277–343.

[11] Karl D. Stephan and Paul F. Goldsmith, "W-band quasioptical integrated PIN diode switch," *1992 IEEE MTT-S Intl. Microwave Symp. Dig.*, Albuquerque, NM, June 1–5, 1992, pp. 591–594. (Preliminary monolithic data presented at conference.)

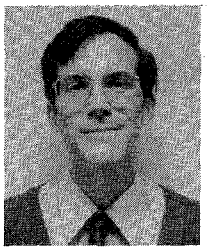

Karl D. Stephan (S'81–M'83–SM'89) received the B.S. degree in engineering from the California Institute of Technology, Pasadena, in 1976, and the M. Eng. degree from Cornell University, Ithaca NY, in 1977. He received the Ph.D. degree in electrical engineering from the University of Texas at Austin in 1983.

In 1977, he joined Motorola, Inc. From 1979 to 1981 he was with Scientific-Atlanta, where he engaged in research and development pertaining to cable television systems. In September, 1983, he joined the faculty of the University of Massachusetts at Amherst, where he is presently Associate Professor of Electrical Engineering. His current research interests include the application of quasi-optical techniques to millimeter wave circuits and subsystems.

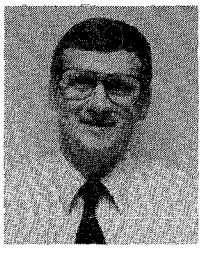

Frank H. Spooner was a Senior Process Engineer at Millitech Corporation responsible for the process development of GaAs devices. He is now with American Holographic. In 1968 he received an Associate Degree in Chemical Engineering from Franklin Institute of Boston.

Since that time he has been the coauthor of three patents and seven articles related to GaAs technology. Prior to joining Millitech, he worked for Alpha Industries, Sperry Research Center and Raytheon Company-Research Division.

Paul F. Goldsmith (M'75–SM'89–F'91) for a photograph and biography, see this issue, p. 1674.